HEAT TRANSFER WITH EVAPORATION AND BOILING OF LIQUID IN THE EVAPORATOR CHANNELS. II.

L. L. Vasil'ev, A. N. Abramenko, and L. E. Kanonchik

UDC 536.423.1

On the basis of results of preliminary tests, described earlier, the authors have constructed a physical model of the channel evaporator.

Physical Model of the Evaporator. This model is based on the following conditions: 1) the channels have a regular geometric form; 2) the liquid moves in the channel only because of surface tension forces; 3) the capillary pressure in the channel is equal to the difference in the equivalent minisci of the liquid; 4) the working liquid practically fully wets the channel material; 5) the transverse meniscus is replaced by the nominal width of the liquid layer; 6) in a triangular channel with maximum heat removal at the initial section the nominal width of the liquid layer is equal to the channel width, and tends to zero at the end section; 7) in a rectangular channel with maximum heat removal at the initial section the equivalent miniscus is flat, and is equal to half the channel width at the end section; 8) the heat removal is hyperbolic along the channel; 9) the liquid flow is laminar; 10) the vapor pressure above the liquid is constant; 11) there is no heat transfer between the dry walls of the evaporator and the vapor; 12) at any cross section of the liquid flow in the channel the capillary pressure increment is equal to the increment of hydraulic resistance.

Theoretical Formula for the Maximum Heat Flux. Triangular Channel

Constant Channel Width. The derivation of the formula is based on the variation of capillary pressure being equal to the hydraulic drag at any cross section of the liquid flow in the channel

$$\frac{dP_{\text{cap}}}{dx} = -\frac{dP_{\text{h}}}{dx}. \tag{1}$$

The capillary pressure in a triangular channel is

$$dP_{\text{cap}} = \sigma dM = -\sigma\cos\theta\frac{dR(x)}{R^2(x)} = -\frac{\sigma\cos\theta\, dt}{t^2(x)\,C_1(\alpha)}. \tag{2}$$

According to the Hagen–Poiseuille law, the hydraulic resistance is

$$dP_{\text{h}} = \frac{f\dot{m}(x)\,\mu_l}{A(x)\,D_{\text{h}}^2(x)\,\rho_l}dx. \tag{3}$$

The mass flux of liquid in the channel at any section can be represented as the difference between the flux of all the liquid vaporized and the flux vaporized in the section from $X = x_0$ to $X = x_0 + x$:

$$\dot{m}(x) = \frac{Q_0'}{r^*}x_0\ln\frac{x_0 + x_{\max}}{x_0 + x}. \tag{4}$$

At the same time, we have

$$\frac{Q_0'}{r^*}x_0\ln\frac{x_0 + x_{\max}}{x_0} = \frac{q_{\max}x_{\max}t}{r^*}. \tag{5}$$

A. V. Lykov Institute for Heat and Mass Transfer, Academy of Sciences of the Belorussian SSR, Minsk. Translated from Inzhenerno-Fizicheskii Zhurnal, Vol. 39, No. 5, pp. 826-832, November, 1980. Original article submitted November 12, 1979.

 0022-0841/80/3905-1198$07.50 © 1981 Plenum Publishing Corporation

Then the variation in resistance along the channel is

$$dP_h = \frac{q_{max} x_{max} t f \mu_l}{r^* \rho_l t^4(x) C_2(\alpha) C_3^2(\alpha)} \frac{\ln \frac{x_0 + x_{max}}{x_0 + x}}{\ln \frac{x_0 + x_{max}}{x_0}} dx. \quad (6)$$

We equate Eqs. (2) and (6) and integrate

$$\frac{\sigma \cos\theta}{C_1(\alpha)} \int_0^t t^2(x)\, dt = \frac{q_{max} t f \mu_l}{r^* \rho_l C_2(\alpha) C_3^2(\alpha)} \int_0^{x_{max}} \frac{\ln \frac{x_0 + x_{max}}{x_0 + x}}{\ln \frac{x_0 + x_{max}}{x_0}} dx. \quad (7)$$

After integrating we have

$$q_{max} = \frac{t^2 r^* \rho_l \sigma \cos\theta C_3^2(\alpha) C_2(\alpha)}{3 f C_1(\alpha) \mu_l x_{max} \left[\frac{(x_0 + x_{max})}{\ln \frac{x_0 + x_{max}}{x_0}} - x_0 \right]}. \quad (8)$$

Since, for a given channel shape, the friction factor depends mainly on the angle α, we introduce the following coefficient:

$$K(\alpha) = \frac{1}{3f}. \quad (9)$$

In addition, we designate

$$N_l = \frac{r^* \rho_l \sigma}{\mu_l}, \quad (10)$$

$$C(\alpha) = \frac{C_3^2(\alpha) C_2(\alpha)}{C_1(\alpha)}. \quad (11)$$

Finally, Eq. (8) takes the form

$$q_{max} = \frac{t^2 N_l \cos\theta C(\alpha) K(\alpha)}{x_{max} \left[\frac{(x_0 + x_{max})}{\ln \frac{x_0 + x_{max}}{x_0}} - x_0 \right]}. \quad (12)$$

Constant Channel Depth. In this case we determine the optimal angle α for which maximum heat removal is achieved. With d = const we write Eq. (12) as

$$q_{max} = \frac{d^2 N_l \cos\theta (1 - \sin\alpha) \sin\alpha K(\alpha)}{x_{max} \left[\frac{(x_0 + x_{max})}{\ln \frac{x_0 + x_{max}}{x_0}} - x_0 \right] (1 + \sin\alpha)^2}. \quad (13)$$

The function $q_{max} = \varphi(\alpha)$ has a maximum at the point $\alpha = 19°$ ($2\alpha = 38°$).

Rectangular Channel. As in the previous case, derivation of the theoretical formula is based on equality of the variation of capillary pressure and hydraulic drag:

$$dP_{cap} = \sigma d\left(2 \frac{\cos\theta}{t}\right) = -\frac{2\sigma}{t} \sin\theta d\theta, \quad (14)$$

$$P_{cap} = -\frac{2\sigma}{t} \int_{\theta=0°}^{\theta=90°} \sin\theta d\theta = \frac{2\sigma}{t}, \quad (15)$$

$$P_h = \frac{f q_{max} x_{max} \mu_l}{4 t^2 \rho_l r^*} \int_0^{x_{max}} \frac{[t + b(x)]^2 \ln \frac{x_0 + x_{max}}{x_0 + x}}{b^3(x) \ln \frac{x_0 + x_{max}}{x_0}} dx. \quad (16)$$

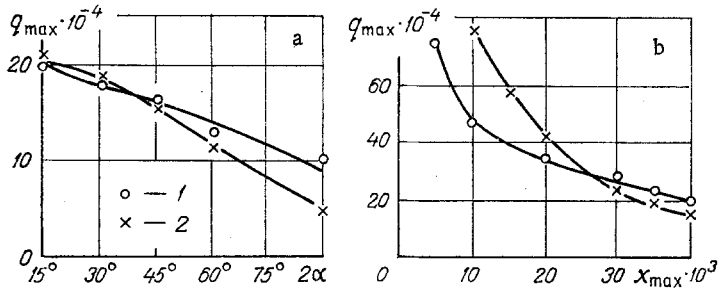

Fig. 1. Maximum heat flux density as a function of: a) the channel vertex angle, $q_{max}\cdot10^{-4}$ W/m², α, in deg; $x_{max} = 40\cdot10^{-3}$ m; $t = 0.4\cdot10^{-3}$ m; b) the channel length, $q_{max}\cdot10^{-4}$ W/m²; $x_{max}\cdot10^{3}$ m, $t = 0.4\cdot10^{-3}$ m; $2\alpha = 30°$ (1 is experiment; 2 is theory).

In the general case the expression for the maximum heat flux has the form

$$q_{max} = -\frac{tN_l K(d)}{x_{max} I}(\cos\theta_{x_0+x_{max}} - \cos\theta_{x_0}), \tag{17}$$

where

$$I = \int_0^{x_{max}} \frac{\left[t + d\left(1 - \frac{x_{max}}{x} K\right)\right]^2}{d^3\left(1 - \frac{x_{max}}{x} K\right)^3} B dx; \tag{18}$$

$$B = \frac{\ln\frac{x_0 + x_{max}}{x_0 + x}}{\ln\frac{x_0 + x_{max}}{x_0}}; \tag{19}$$

$$K = \frac{\ln\frac{x_0 + x}{x_0} + \sum_{i=1}^{n}(n-i)\ln\frac{x_0 + x_i}{x_0 + x_{i-1}}}{\ln\frac{x_0 + x_{max}}{x_0} + \sum_{i=1}^{m}(m-i)\ln\frac{x_0 + x_i}{x_0 + x_{i-1}}}; \tag{20}$$

$$K(d) = \frac{8}{f}. \tag{21}$$

The numerical value of I has a minus sign.

In the theoretical formulas (12), (13) and (17) there is a term $x_0 = 10^{-2}$ m. It should be regarded as a constant factor, determined by the structure of the experimental evaporator element. In heat pipes the section of channel occupied by the artery connector is so small that it can be neglected. Therefore, in designing evaporators according to the above formulas (12), (13), and (17) we should consider that x_{max} is the entire channel length, and that $x_0 = 10^{-2}$ is a constant coefficient.

Comparison of Experimental and Theoretical Results. During the experiments we recorded the heat flux density as a function of the channel wall overheat above the saturation temperature. The heat flux increased with increase of ΔT_{av}. At low overheat (5-10°K) heat was removed by evaporation. By eye we observed unperturbed flow of liquid along the channel, and we clearly tracked its penetration along the length. With further increase in overheat the process of bubble formation in the liquid flow began. Since the vapor pressure in a bubble is higher than the saturation pressure, bubble breakdown is accompanied by sputtering of liquid. With increase of overheat the sputtering intensity increases, so that it is a qualitative measure of the heat removal intensity in the channel. However, the intensification of heat removal with increase of overheat is not unbounded. At a certain value of ΔT_{av} the heat flux density reaches a maximum, since the rate of heat supply is equal to the maximum possible rate of removal achieved by the channel. The higher is the mass flow rate of working liquid in the channel, the larger is the power that it can dissipate.

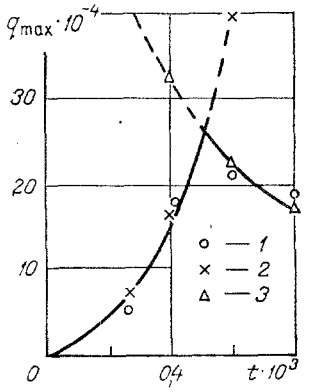

Fig. 2

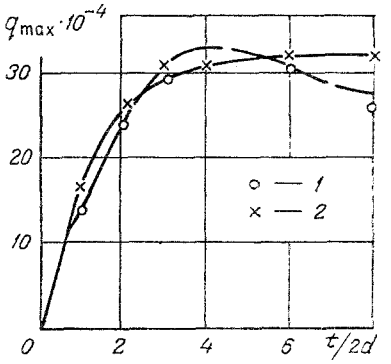

Fig. 3

Fig. 2. Maximum heat flux density as a function of the width of a triangular channel: $x_{max} = 40 \cdot 10^{-3}$ m, $2\alpha = 30°$ [1) experiment; 2) theory; 3) transmission capibility of the arteries]. $q_{max} \cdot 10^{-4}$, W/m², $t \cdot 10^3$, m.

Fig. 3. Maximum heat flux density as a function of the depth/width ratio of a triangular channel: $x_{max} = 40 \cdot 10^{-3}$ m, $t = 0.4 \cdot 10^{-3}$ m [1) experiment; 2) theory]. $q_{max} \cdot 10^{-4}$ W/m², 2d/t.

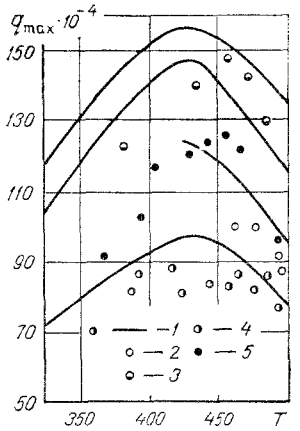

Fig. 4. Comparison of the results with the data of Marits: 1) theory; 2, 3, 4, 5) pipes of 19/1, 19/2, 20/1, 20/2, respectively. $q_{max} \cdot 10^{-4}$, W/m², T, K.

For triangular channels the width of the base of the triangle was varied from $0.25 \cdot 10^{-3}$ to $0.8 \cdot 10^{-3}$ m, the vertex angle from 15 to 90°, and the length of the evaporator section from $5 \cdot 10^{-3}$ to $40 \cdot 10^{-3}$ m. From the experimental results we determined that (Fig. 1a)

$$K(\alpha) = 0.0535 (2\alpha)^{1.55}. \quad (22)$$

The investigations conducted have confirmed the basic premise of the physical model that the heat removal is hyperbolic along the channel length. A decrease of the length of the evaporator section of the channel from $40 \cdot 10^{-3}$ to $5 \cdot 10^{-3}$ m caused an increase in the heat flux by more than a factor of 4, while for uniform heat removal the degree of increase should be 64. It should be noted that the heat flux density in the channel at $x_{max} = 5 \cdot 10^{-3}$ m exceeded the critical value for a large volume [1]. This is explained by it being impossible to form a stable vapor film because the channel height exceeded the separation diameter. In the supercritical zone the experimental heat flux density is below the theoretical. Probably the increase of bubble formation and the formation of dry spots on the channel wall create added resistance to flow of the working liquid (Fig. 1b).

An increase in channel width caused an increase in the flow rate of liquid passing along it. Therefore, the heat transfer was intensified. However, the increase in channel width correspondingly increases the channel equivalent radius, leading to a reduced capillary pressure driving the liquid along the arteries (Fig. 2).

The results of experiment and theory for a channel whose angle varied from 15 to 90° are shown in Fig. 1a. With increase of angle there is reduced transmission cross section of channel, and therefore the heat removal drops in intensity. Experiment and theory show good agreement in the region of angle values from 15 to 60°. For 90° the experimental heat flux is considerably above the theoretical. For the large angles there is a sharp fall in the capillary head and the process of liquid sputtering upon boiling is the dominant influence on the heat transfer.

For the rectangular channels the experimentally determined coefficient K(d) was

$$K(d) = 14.5\frac{t}{2d}. \tag{23}$$

The authors investigated evaporators with channels of constant width ($t = 0.4 \cdot 10^{-3}$ m) and length ($x_{max} = 40 \cdot 10^{-3}$ m), whose depth varied from $0.2 \cdot 10^{-3}$ to $1.6 \cdot 10^{-3}$ m. An increase of depth led to an increase in the transmission section of the channel and to intensification of circulation of acetone. However, it is difficult for a vapor bubble to escape in a channel whose depth is too great, and it therefore slows down the rate of liquid motion. This leads to a considerable reduction in heat removal in channels that are too deep (Fig. 3).

The data calculated from Eq. (12) are compared with the experiment of Marits [2] in Fig. 4. It can be seen that theory and experiment agree satisfactorily (the maximum difference is 25%).

The calculated values of the optimal vertex angle ($2\alpha = 38°$) for a triangular channel of constant depth agree well with the computed values ($2\alpha = 30°$) of Bresler and White [3].

NOTATION

A(x), area of the transverse liquid layer in the channel at section x, m^2; B, a factor accounting for the ratio of the current length to the total length of a rectangular channel; b(x), height of the liquid layer at section x, m; D_h, hydraulic diameter of the liquid flow in the channel at section x, m; d, channel depth, m; $C(\alpha)$, constant for a given value of α; $C_1(\alpha)$, a constant defining R(x); $C_2(\alpha)$, a constant defining A(x); $C_3(\alpha)$, a constant defining D_h; f, friction factor; I, a definite integral; K, a coefficient; $K(\alpha)$, flow friction coefficient in a triangular channel; K(d), friction coefficient in a rectangular channel; m(x), mass flux of liquid in the channel at section x, m^3/sec; M, meniscus, 1/m; N_l, a characteristic of the working liquid; P, pressure, N/m^2; Q, heat flux, W; Q_0', height of hyperbola at the point x_0, W/m; q, heat flux density, W/m^2; R, meniscus radius, m; r*, latent heat of vaporization, J/kg; T, temperature, °K; t, channel width, m; x, y, coordinates; α, semiangle at vertex of a triangular channel, deg; θ, wetting angle, deg; μ, viscosity, $N \cdot sec/m^2$; ρ, density, kg/m^3; σ, surface tension, N/m. Subscripts: h, hydraulic; l, liquid; cap, capillary; 0, initial; max, maximum; av, average; x, coordinate of channel section.

LITERATURE CITED

1. L. Tong, Heat Transfer with Boiling and Two-Phase Flow [Russian translation], Mir, Moscow (1969), pp. 54-55.
2. K. Marits, "Influence of capillary geometry on heat transfer," in: Heat Pipes [Russian translation], Mir, Moscow (1972), pp. 32-117.
3. R. Bresler and P. White, "Wetting of a surface by means of capillary channels," Teploperedacha, 92, No. 2, 126-132 (1970).